Framework for discrete-time quantum walks and a symmetric walk on a binary tree

Zlatko Dimcovic,[1, *] Daniel Rockwell,[2] Ian Milligan,[2] Robert M. Burton,[2] Thinh Nguyen,[3] and Yevgeniy Kovchegov[2]

[1]*Department of Physics, Oregon State University, Corvallis OR 97331*
[2]*Department of Mathematics, Oregon State University, Corvallis OR 97331*
[3]*School of Electrical Engineering and Computer Science, Oregon State University, Corvallis OR 97331*
(Dated: July 18, 2011)

We formulate a framework for discrete-time quantum walks, motivated by classical random walks with memory. We present a specific representation of the classical walk with memory 2 on which this is based. The framework has no need for coin spaces, it imposes no constraints on the evolution operator other than unitarity, and is unifying of other approaches. As an example we construct a symmetric discrete-time quantum walk on the semi-infinite binary tree. The generating function of the amplitude at the root is computed in closed-form, as a function of time and the initial level n in the tree, and we find the asymptotic and a full numerical solution for the amplitude. It exhibits a sharp interference peak and a power law tail, as opposed to the exponentially decaying tail of a broadly peaked distribution of the classical symmetric random walk on a binary tree. The probability peak is orders of magnitude larger than it is for the classical walk (already at small n). The quantum walk shows a polynomial algorithmic speedup in n over the classical walk, which we conjecture to be of the order 2/3, based on strong trends in data.

I. INTRODUCTION

Random walks on graphs (Markov chains) are used extensively in science. They provide a number of now standard approaches and models in physics. Application of such ideas to evolution of quantum systems has led to the emergence of the field of *quantum walks*, principally distinguished between discrete-time (DTQW) and continuous-time (CTQW) walks. However, being unitary (reversible) processes, quantum walks are very different from their classical stochastic (Markovian) counterparts.

Quantum walks are used to approach varied problems, for instance, on quantum lattice gases, arrow of time, generalized quantum theory, exciton trapping, topological phases [1–5]. They may become a general tool for building physical models; for example, see a summary in [5] and CTQW in transport phenomena [6]. In quantum computing, they are a universal primitive [7], and in the algorithmic context the principle alternative to quantum Fourier transform. The field has developed since its initiation [8–12], with established algorithmic uses, examples of dramatic superiority over classical approaches [13, 14], and implementations [15]. See [16, 17] for a review and a recent summary.

Standard approaches to quantum walks generally stem from memoryless classical walks. However, since quantum evolution is memoried (unitary), it seems natural to approach construction of quantum walks from classical random walks with memory. Relation between unitarity and memory in walks has been noted [1, 3]. (Also, in computer science memoried and biased approaches are common and beneficial algorithmically.)

It is our observation that DTQW are most directly related to classical walks with memory 2. In this paper we present a general DTQW framework as a direct analog of a specific representation of memory–2 classical walks. With it we construct a symmetric DTQW on a binary tree, starting from a pure state at an arbitrary level in the tree, and compute its amplitude at the root.

Sec. II starts with a representation for memoried classical walks, that is particularly interesting for quantum walks due to the specific form of the Markov tensor. In an analogy with it, we then define a framework for DTQW. Walks are built by choosing the evolution operator with no constraints other than unitarity. They evolve in the product of state spaces, while the key component of the operator acts on single states. There is no need for "coin" degrees of freedom. The framework is flexible and suitable for general graphs. It is also unifying of other approaches, notably coined and Szegedy's [18].

In Sec. III we apply this framework to a binary tree, a structure with many uses in physics. It is a natural environment for quantum walks, but difficult to utilize with current techniques for DTQW. A successful specific construction exists for CTQW [13].

We construct a symmetric walk on the semi-infinite binary tree, and calculate its amplitude at the root, as a function of time and of the initial level in the tree. This involves path enumeration using regeneration structures, manipulated with the z–transform. The obtained closed–form generating function yields the analytic asymptotic for the amplitude, which we also compute numerically. The amplitude has a sharp peak and a power law tail, completely unlike the corresponding classical random walk, and shows a polynomial speedup in n. The data strongly suggests the order of the speedup of 2/3.

A summary is in Sec. IV, and appendices discuss the steepest descent calculation, and the classical walk.

* dimcoviz@onid.orst.edu

II. A FRAMEWORK FOR DISCRETE-TIME QUANTUM WALKS

The main approach to DTQW follows ideas of classical memoryless walks, and needs an auxiliary "coin" degree of freedom. Here we employ a specific representation of memoried Markov chains (II A), as an analogy for a general DTQW framework (II B) which does not need coin spaces. Relation to other approaches is discussed in closing of this section. We start with an example that serves as a motivation for using memoried walks.

Memoried walks and coined DTQW. Classical walks with memory are walks with internal states: apart from its state, the walk carries other information. Here we use one such walk in 1 dimension, with the following property: the next step depends on the *direction* of the previous one. If the walker came to a site i from the site $i-1$, the probability to go to $i+1$ (to maintain the direction) is p, while the probability to go to $i-1$ (reverse direction) is $1-p$. This is often called a *persistent* walk. We now show that coined DTQW are a special case of a quantum analog of classical persistent walks.

Consider a standard coined walk on a d–regular graph with n vertices (for example, [12]). The state of the walk is in the direct product of two Hilbert spaces: an auxiliary ('coin') space $\mathcal{H}_A$, spanned by d states $|a\rangle$, in which a unitary operator C mixes components; and a space of vertices, $\mathcal{H}_V$, spanned by n states $|v\rangle$. The evolution operator acts in this product space $\mathcal{H}_A \otimes \mathcal{H}_V$ as: $U(|a\rangle \otimes |v\rangle) = S(C \otimes I)(|a\rangle \otimes |v\rangle)$. On a cycle with the $\mathcal{H}_A$ basis $\{|\uparrow\rangle, |\downarrow\rangle\}$, the shift S can be implemented as $S = |\uparrow\rangle\langle\uparrow| \otimes \sum_j |j+1\rangle\langle j| + |\downarrow\rangle\langle\downarrow| \otimes \sum_j |j-1\rangle\langle j|$. Now consider for C a generalized Hadamard coin operator,

$$C = \begin{bmatrix} \sqrt{p} & \sqrt{1-p} \\ \sqrt{1-p} & -\sqrt{p} \end{bmatrix},$$

and evolve the state. Starting from the pure 'up' state,

$$\begin{aligned} &S \cdot (C \otimes I) |\uparrow\rangle \otimes |i\rangle \\ &= S \cdot \left(\sqrt{p} |\uparrow\rangle \otimes |i\rangle + \sqrt{1-p} |\downarrow\rangle \otimes |i\rangle \right) \\ &= \sqrt{p} |\uparrow\rangle \otimes |i+1\rangle + \sqrt{1-p} |\downarrow\rangle \otimes |i-1\rangle. \end{aligned} \quad (1)$$

For the pure 'down' initial state,

$$\begin{aligned} &S \cdot (C \otimes I) |\downarrow\rangle \otimes |i\rangle \\ &= \sqrt{1-p} |\uparrow\rangle \otimes |i+1\rangle - \sqrt{p} |\downarrow\rangle \otimes |i-1\rangle. \end{aligned} \quad (2)$$

This is a persistent walk: it maintains the direction with probability p, and changes it with probability $1-p$. The obtained walk undergoes the same spectral analysis as its unbiased special case ($p = 1/2$, the Hadamard walk). General coin has been studied (for example, [19–22]), as well as persistent (correlated) walks and their relation to DTQW [23–25]. With this example we point out the direct correspondence between them. Note that the directionality of the walk shows up as soon as the coin transformation is allowed to have $p \neq 0.5$. In other words,

the standard Hadamard transform generally implements a persistent walk (rather than a memoryless one), only with equal probabilities.

A. A representation for classical memory–2 walks

Walks with memory 2 are such Markov processes where the next step depends on two states: the current one, and the previous one. Walks with memory are generally studied by using a suitably enlarged state space. In particular, a memory–2 Markov chain can be represented as a memoryless one over the space with n^2 states. The transition matrix is then large ($n^2 \times n^2$) and sparse.

Instead, here we represent a Markov chain with memory k by a probability distribution $\mu(t)$ of dimension k, while the Markov tensor $\mathcal{M}$ is then of dimension $k+1$. For a memory–2 walk over n sites, the space has dimension n, and each state is labeled by two indices (the site the walker came from, and the current site). So the probability distribution is 2–dimensional,

$$\mu(t) = \begin{bmatrix} \mu_{0,0}(t) & \cdots & \mu_{0,n-1}(t) \\ \vdots & & \vdots \\ \mu_{n-1,0}(t) & \cdots & \mu_{n-1,n-1}(t) \end{bmatrix}.$$

The matrix μ_{ij} can also be given by a column of rows r_i, or by a row of columns c_i, what we will use shortly. The following representation for the third-rank tensor $\mathcal{M}$ and its action is convenient.

Let $p_{ij|k}$ be the conditional probability for the transition $j \to k$, given that the walk came to j from i. All transition probabilities $\{p_{ij|k}\}$ define the evolution operator $\mathcal{M} = [P_0 P_1 \ldots P_{n-1}]$, as n layers of $n \times n$ transition matrices P_j, $j = 0, 1, \ldots, n-1$, one for each site:

$$P_j = \begin{bmatrix} p_{0,j|0} & p_{0,j|1} & \cdots & p_{0,j|n-1} \\ \vdots & & & \vdots \\ p_{n-1,j|0} & p_{n-1,j|1} & \cdots & p_{n-1,j|n-1} \end{bmatrix}.$$

P_j are by construction transition probability matrices, and this is the only requirement imposed on them.

The evolution of the state, $\mu_{t+1} = \mu_t \mathcal{M}$, with $\mathcal{M}$ acting to the left, is defined as

$$\mu(t) \mapsto \mu(t+1) : \ r_j(t+1) = c_j^\mathsf{T}(t)P_j,$$

for each $j = 0, 1, \ldots, n-1$, where r_j and c_j^T are the j-th row and transposed column, respectively, of the matrix μ. In words: *at each site j, the P_j associated with that site acts on the transposed j–th column of $\mu(t)$, giving the j–th row of the evolved $\mu(t+1)$.*

Instead of an $n^2 \times n^2$ probability matrix, we use n of $n \times n$ probability matrices P_j. They implement the evolution: the j–th column of $\mu(t)$ has probabilities to arrive to j from any site, and after the action of P_j the j–th row of $\mu(t+1)$ has probabilities to go from j to any site. Thus action of all transition matrices on all columns evolves

the probability distribution over all paths. The stochastic nature of the process is carried by the assignment of $\{p_{ij|k}\}$ transition probabilities in P_j matrices [26].

The P_j transition matrices are simple in most cases of interest. Consider the cycle, a space $\{0, 1, \ldots, n\}$ with identified ends $(0$ and $n)$, with only nearest-neighbor transitions, $(j \pm 1, j) \rightarrow (j, j \pm 1)$. Take the persistent walk, with probability p to continue, and $1 - p$ to reverse,

$$(j - 1, j) \rightarrow (j, j + 1), \quad \text{with probability } p$$
$$(j - 1, j) \rightarrow (j, j - 1), \quad \text{with probability } 1 - p.$$

To obtain this walk, the P_j matrices have the following block centered at $(j, j) \pmod{n}$,

$$P_j \;=\; \begin{bmatrix} \ddots & & & & & & \\ & 1 & & & & & \\ & & 1-p & 0 & p & & \\ & & 0 & 1 & 0 & & \\ & & p & 0 & 1-p & & \\ & & & & & 1 & \\ & & & & & & \ddots \end{bmatrix} \tag{3}$$

The rest of the diagonal of P_j has 1s, other elements are 0, except for the transitions between sites $0 \equiv n$, and $n-1$ or 1 (boundary conditions), which are $p_{0,n-1|0} = 1 - p$ (reverse), $p_{0,n-1|1} = p$ (continue), etc. Action of these P_j by the above prescription carries the walk.

B. Quantum walks: the interchange framework

The above classical procedure for memory–2 walks is directly elevated to define quantum processes.

Consider a basis in an N–dimensional Hilbert space, with vectors labeled as $\{|i\rangle, i = 1, 2, \ldots N\}$. They represent states that the walk is performed on, enumerated on a general graph. The state of the walk is given in the product $\mathbb{C}^N \times \mathbb{C}^N$ spanned by these bases, by states at the previous $(|i\rangle)$ and current $(|j\rangle)$ step,

$$|\psi(t)\rangle = \sum_{ij} c_{ij}(t) \, |i\rangle \otimes |j\rangle. \tag{4}$$

The evolution is specified by

$$|\psi(t+1)\rangle = \widehat{U}\widehat{X} \, |\psi(t)\rangle, \quad |\psi(t)\rangle = (\widehat{U}\widehat{X})^t \, |\psi(0)\rangle, \tag{5}$$

where $\widehat{X}$ is the interchange operator, and $\widehat{U}$ is defined via unitary operators U_j in $\mathbb{C}^N$, assigned for each site,

$$\widehat{X} \colon \; |i\rangle \otimes |j\rangle \mapsto |j\rangle \otimes |i\rangle$$
$$\widehat{U} = \sum_{j=0}^{N-1} \Pi_j \otimes U_j, \quad \text{where} \quad \Pi_j = |j\rangle\langle j|. \tag{6}$$

Π_j selects the first state in the product, and U_j acts on the second. Before explicit examples, we make a few general comments.

Consider a pure state of the walk, $|i\rangle \otimes |j\rangle$, represented by an arrow pointing from the previous (i) to the current (j) site. The interchange initiates the walk forward by 'reversing the arrow.' Then the U_j operator distributes the 'tip of the arrow' to all sites the process can access (generally in the subspace of adjacent nodes), and the evolved superposition is obtained. This is best seen in the forthcoming example of the binary tree (Fig. 2). The explicit reversal $\widehat{X}$ is crucial: then U_j completely control the evolution over site j, by acting on the originating state(s) $|i\rangle$, and sending the process over all paths to a new state. The framework does not place any conditions on these operators, except for unitarity of quantum evolution. We are free to choose (or construct) them as needed to implement quantum walks.

Note that this construction needs no mention of classical processes. The representation of classical memoried walks in Sec. II A is given for motivation and insight, and we now comment on this relation. The discussed interplay between interchange and (local) U_j, critical for this formulation, has a clear analog in the classical representation—recall the transposition before (local) P_j evolve the distribution. Also, the freedom to craft any (unitary) U_j to implement quantum walks corresponds to a classical property, as P_j may be any (probabilistic) matrices. Finally, the classical representation has no explicit coin toss, and there is no need in the quantum case to mimic randomization via a coin degree of freedom; here U_j drive the walk and mix components.

Relation to other approaches. For a comparison with a memoryless (coined) approach, consider a walk on the line, over the state space $S = \{|j\rangle, j = 0, 1, \ldots\}$. The quantum walk (1–2) is obtained with

$$U_j(p) = \begin{bmatrix} \ddots & & & & & & \\ & 1 & & & & & \\ & & \sqrt{1-p} & 0 & \sqrt{p} & & \\ & & 0 & 1 & 0 & & \\ & & -\sqrt{p} & 0 & \sqrt{1-p} & & \\ & & & & & 1 & \\ & & & & & & \ddots \end{bmatrix}, \quad \begin{array}{l} \text{centered} \\ \text{at } (j, j). \end{array}$$

The rest of the diagonal has 1s, other elements are 0. (On a cycle there are elements needed for boundary conditions, like in the classical case.) The square roots provide for probability being the square of the amplitude, the $-\sqrt{p}$ sign is needed for unitarity. In this simple case, the choice of U_j follows from the classical memoried walk (3), but in general a classical analog is not needed.

Now look at the evolution steps from pure states. Starting from $|i-1\rangle \otimes |i\rangle$ (the system is in the state $|i\rangle$, having been in $|i-1\rangle$ at the previous step),

$$\widehat{U}\widehat{X} \, |i-1\rangle \otimes |i\rangle = \widehat{U} \, |i\rangle \otimes |i-1\rangle$$
$$= \Big(\sum_{j \in S} |j\rangle\langle j| \otimes U_j \Big) |i\rangle \otimes |i-1\rangle$$
$$= \sqrt{1-p} \, |i\rangle \otimes |i-1\rangle + \sqrt{p} \, |i\rangle \otimes |i+1\rangle.$$

Similarly, for the initial $|i+1\rangle \otimes |i\rangle$ state,

$$\widehat{U}\widehat{X}|i+1\rangle \otimes |i\rangle = -\sqrt{p}\,|i\rangle \otimes |i-1\rangle + \sqrt{1-p}\,|i\rangle \otimes |i+1\rangle.$$

This is an isomorphism of the memoryless–based walk (1–2), via identification

$$|i-1\rangle \otimes |i\rangle \Leftrightarrow |{\uparrow}\rangle \otimes |i\rangle \quad \text{and} \quad |i+1\rangle \otimes |i\rangle \Leftrightarrow |{\downarrow}\rangle \otimes |i\rangle.$$

This analysis applies to arbitrary mixed states, as each component is evolved separately. The choice of $p = 1/2$ restores Hadamard walk. Thus the interchange framework reproduces coined quantum walks on the line directly, with the above choice for U_j.

Memory in quantum walks is mentioned in literature. For example, it was noted in study of the classical limit via decoherence and multiple coins [27], and a direct relation between coined walks and classical memoried walks was observed [28]. Recently a particular "quantum walk with memory" [29] was studied.

An important approach directly resorting to ideas of memoried walks is Szegedy walk [18], which is the most prominent tool in DTQW not using coin degree of freedom [17]. Its construction starts from a classical Markov chain, and the resulting evolution operator explicitly carries classical transition probabilities. It is contained in the interchange framework via the specific choice

$$(U_j)_{km} = 2\sqrt{p(j,i_k)p(j,i_m)} - \delta_{km},$$

where $p(i,j)$ need be classical transition probabilities. The present approach does not require a specific form of the evolution operator. It is fully defined by (4–6) alone, without reference to classical walks, and quantum processes with desired properties are set by choosing U_j without constraints. Some benefits of this are seen in the next section, where we construct a symmetric DTQW on a binary tree. A Szegedy walk on a binary tree cannot be obtained with equal probabilities for each branch, as there is no (real) solution for probabilities $p(i,j)$ such as to yield $1/3$ probability for the quantum walk.

Szegedy walk is also a translation of a memoryless walk into a walk with memory. The interchange framework is a direct analog of an explicit representation for memory–2 Markov chains. This is reflected in some of its properties, discussed above.

The interferometry–motivated [30] scattering walk [31] is performed on graph edges, scattering off of vertices (or subgraphs). The more general formulation [32] can be formally reconciled with the present framework, while their designs and interpretations are different, and complementary. Scattering walk has recently been used, in its form reflecting the physical (scattering) approach, for certain search problems [32–34], hinting at benefits of coinless algorithms. This approach has not been related to stochastic processes, which underlie the motivation, construction, and expected uses of the present framework. We showed here how a very general formulation of DTQW, unifying of other similar approaches [35], arises naturally from Markov chains with memory.

Before moving to a full example we remark on the versatility of this approach. It reproduces coined walks on the line and Szegedy's walk, handles a walk on a binary tree (next section)—each by a simple choice for U_j. This demonstrates flexibility, and it seems that the framework can help with problems so far prohibitively difficult.

III. A SYMMETRIC DISCRETE-TIME QUANTUM WALK ON A BINARY TREE

Binary tree is a common model in physics, and a structure of interest in quantum computing [36]. One of the initiating works [8] used it as a model for decision trees, and one of the most successful algorithms [13] solves a particular problem on connected binary trees—both using CTQW. We have not seen such progress in using DTQW on the binary tree, even though this would be beneficial for many problems. This seems to be due mostly to trouble in handling coin spaces that are necessary for (coined) DTQW. In this section we use the established framework to set and calculate a symmetric DTQW on the semi-infinite binary tree. We orient our tree with the root (single starting node) at the left, with the tree spanning to the right, Fig. 1.
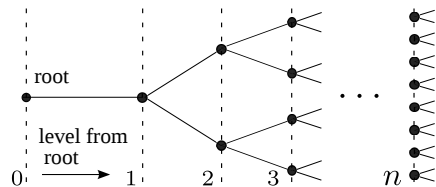
FIG. 1. Conventions used for our binary tree.

We focus on the following basic question. The walk is started from a pure state at a site in the tree at a level n, and we examine its amplitude at the root as a function of time (step) and the initial distance n.

The desired symmetric walk has equal probability to step to either of the connecting nodes, having come from either direction. (The analysis remains unchanged for different choices of local U_j.) The state of the walk is given in the direct product of spaces, each spanned by states defined at nodes, $S = \{|i\rangle\}$. Label a node in the tree as j, and the nodes connected to it as i_1 (to its left, toward the root), i_2, and i_3 (to its right, away from the root), as in Fig. 2. Consider an evolution step from a pure state at j, for example $|\psi_0\rangle = |i_2\rangle \otimes |j\rangle$. The action of the interchange $\widehat{X}$ reverses the state. Next we want to write down the U_j matrix, acting on $|i_2\rangle$, such that the evolved state has equal probabilities for either branch. Formally U_j operate in the space of all nodes, but they are reduced to the subspace of nodes to which transitions are allowed; here the adjacent ones. Thus U_j can be written in a block-diagonal form, with the non-trivial transition matrix U_j^{red} in $\{|i_1\rangle, |i_2\rangle, |i_3\rangle\}$, and an identity matrix over the remaining dimensions. The matrix

elements need to satisfy the unitarity of U_j and equal squared amplitudes of components of the state evolved by it. The obtained evolution operator, with (reduced) transition matrix U_j^{red} in the basis $\{|i_1\rangle, |i_2\rangle, |i_3\rangle\}$, is

$$U_j = \begin{bmatrix} U_j^{\text{red}} & 0 \\ 0 & \mathbb{I} \end{bmatrix}, \quad \text{with} \quad U_j^{\text{red}} = \frac{1}{\sqrt{3}} \begin{bmatrix} 1 & a & a \\ a & 1 & a \\ a & a & 1 \end{bmatrix}, \quad (7)$$

where $a = e^{2\pi i/3}$. This representation holds for graphs of any degree, where dimensions of U_j^{red} and $\mathbb{I}$ change. At the root the walk can only get reflected, what is performed by interchange $\widehat{X}$; then U_0 is the identity matrix. This will be accounted for. For all other states, we now follow the prescription (5–6). With $\widehat{U} = \sum_{i \in S} \Pi_i \otimes U_i$, the step is

$$|\psi_1\rangle = \widehat{U}\widehat{X}|\psi_0\rangle = \left(\sum_{i \in S} |i\rangle\langle i| \otimes U_i \right) \widehat{X}|i_2\rangle \otimes |j\rangle$$

$$= |j\rangle \otimes U_j|i_2\rangle = |j\rangle \otimes \frac{1}{\sqrt{3}} (a, 1, a, 0, \dots)^{\mathsf{T}}. \quad (8)$$

Thus the state is evolved by $\widehat{U}\widehat{X}$ to the superposition

$$|i_2\rangle \otimes |j\rangle \rightarrow |j\rangle \otimes \left(\frac{a}{\sqrt{3}} |i_1\rangle + \frac{1}{\sqrt{3}} |i_2\rangle + \frac{a}{\sqrt{3}} |i_3\rangle \right). \quad (9)$$

Each component of the superposition takes the next step from its node in the same way, and the process spreads over the tree [37].
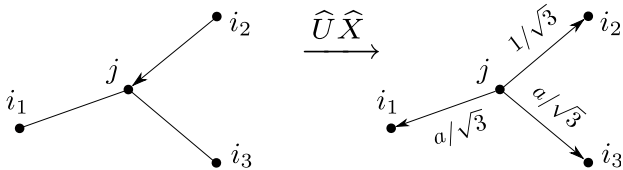
FIG. 2. A step taken from a pure state $|i_2\rangle \otimes |j\rangle$, Eqs. (7–9). The state is sent by $\widehat{U}\widehat{X}$ over all available paths. Probabilities for either branch are chosen to be equal, regardless of how the walk approaches the site j (the walk is symmetric). Each component of a general (mixed) state is evolved this way.

In comparison with Markov processes, a quantum walk can be considered as the evolution of the amplitude distribution. Also, the causality typical of the local dynamics of the classical Markov evolution, seen in Sec. II A, is reflected in the quantum walk. Note how the concerted action of $\widehat{X}$ and U_j implements the 'arrowed' (memoried) nature of the evolution, mentioned in Sec. II B.

For organizing the calculation, it is useful to note the connection between directionality and weights of the components of the evolved state. The component that reverses the direction of the previous step has the coefficient $1/\sqrt{3}$, while the other two have $a/\sqrt{3}$, see Fig. 2. This is always the case for this walk (not only for $|i_2\rangle \otimes |j\rangle$), since it is symmetric, as explicit in Eqs. (7–9).

Outline of the calculation. The amplitude at the root at time t is computed as a sum of the contributions (amplitudes) of all possible (classical) paths that are at the root at that time. This is practically a discrete form of the path integral in quantum mechanics, and is a standard technique [1, 11]. So we count all such classical paths on this structure, weighted appropriately.

The presence of a reflective boundary (the root) complicates the classification and counting, and we use regeneration structures, which are then handled via the z–transform. The obtained explicit expression for the transform is complicated, and analytically the asymptotic of its inverse is found, using the method of steepest descent. The full amplitude is calculated numerically.

For brevity in involved descriptions, we sometimes use "paths $h(t)$" to refer to "those paths that contribute to the part of the amplitude (that is named) $h(t)$."

A. Path counting and regeneration sums

Enumeration of paths, weighted with appropriate coefficients (amplitude), is a combinatorial problem.

Given the symmetry between up and down directions, the tree can be projected to a line bisecting it. The paths on the tree can be classified, and this results in rules for an equivalent walk on that line.

A component of the state at a site is directed either toward or away from the root; and it can either continue in the same direction or reverse it in the next step. For example, the component directed toward the root (to the left) can continue toward the root (taking the branch to the left), with the amplitude $a/\sqrt{3}$, or it can turn and step away from the root, by directly reversing or (and) by taking the other branch leading away, with the total amplitude of $(1 + a)/\sqrt{3}$. See Fig. 2 or Eq. (9).

Summarized by the direction of the previous step, the walk on the line can take the next step as follows:

When directed away from the root (to the right), it can:

— turn back, with the coefficient $1/\sqrt{3}$ (*"left–turn"*);

— continue, with $(a + a)/\sqrt{3}$ (*"right–step"*).

When directed toward the root (to the left), it can:

— turn away, with $(1 + a)/\sqrt{3}$ (*"right–turn"*);

— continue, with $a/\sqrt{3}$ (*"left–step"*).

There is a special case, not following the above classification, which complicates the counting of paths considerably. We need to count weighted paths that are at the root at time t. Paths generally reach the root in fewer than t steps, then going back and forth in the tree, possibly touching the root again in the process, before finally finding themselves at the root at time t. Whenever they touch the root their next step can only be a turn back, with the coefficient 1, and this does not fall into

the above classification. To account for it the paths need be enumerated particularly carefully.

All paths that are at the root at time t have the following structure. They touch the root for the first time at one point (step s), and we call the amplitude for this part of the path $h_n(s)$. Then they go out in the tree, eventually coming back to the root at step t, possibly touching it multiple times in the process; we call the amplitude of this part of the path $G(t - s)$. This is encoded by the convolution over the first contact with the root, and the amplitude, represented by weighted paths that are at the root at step t, starting from level n, is

$$H_n(t) = \sum_{s \geq n}^{t} h_n(s) G(t - s). \tag{10}$$

After the root is touched for the first time, the remainder of the walk is a root–to–root path, considered independently as $G(t)$ (accounting for $n = 0$ case, $G(t) = H_0(t)$). It consists of: a "simple loop" $g(s)$, that goes from the root into the tree and back to it (reaching it again for the first time), followed by the rest of the path $G(t-s)$, which may touch the root multiple times, so again comprised of simple root–to–root loops (Fig. 3).
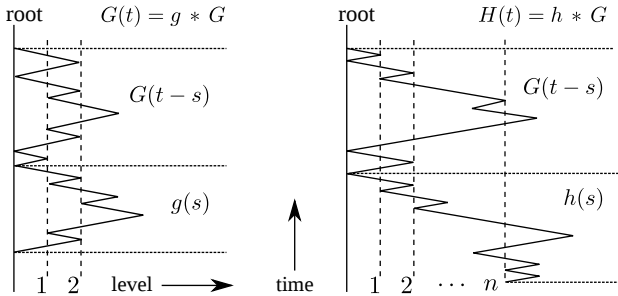
FIG. 3. The number of paths is a convolution w.r.t. the first contact with root, with the regeneration structure (10–11).

This too is a convolution, with one adjustment. To correctly account for $t = 0$, it must be that $g(0) = 0$, as well as $G(0) = 1$ (since $t = 0 \Rightarrow s = t$). Thus $\delta_0(t)$ need be added. The amplitude of such root–to–root multi–loops $G(t)$ is

$$G(t) = \sum_{s=0}^{t} g(s) G(t - s) + \delta_0(t). \tag{11}$$

The regeneration sums (10–11) organize path counting. We work with them using the z–transform,

$$\widehat{f}(z) = \sum_{t=0}^{\infty} f(t) z^t, \quad |z| < 1.$$

Applying this transformation to Eqs. (10) and (11),

$$\widehat{H}_n(z) = \widehat{h}_n(z) \, \widehat{G}(z), \text{ and } \widehat{G}(z) = \widehat{g}(z) \, \widehat{G}(z) + 1,$$

$$\Rightarrow \quad \widehat{H}_n(z) = \widehat{h}_n(z) \, \frac{1}{1 - \widehat{g}(z)}. \tag{12}$$

We need transforms of amplitudes of paths reaching the root for the first time, $\widehat{h}_n(z)$, and of simple loops, $\widehat{g}(z)$.

At this point we note a known combinatorial result. The number of paths on a lattice in two dimensions, going from $(0, 0)$ to $(2n, 0)$, taking only NE or SE steps, with k peaks, is given by Narayana numbers [38],

$$N(n, k) = \frac{1}{n} \binom{n}{k} \binom{n}{k - 1}. \tag{13}$$

This expression applies to the number of paths comprising the simple loops g, where peaks are positions furthest from the root. We first need to identify and enumerate "*steps*" and "*turns*" in such paths, so that we can assign weights to them accordingly.

A simple loop must take an even number of steps. The first step is a reversal: it starts at the root, having arrived to it from the first node, and it can only step back onto the first node, so the coefficient for this step is 1. It is straightforward to establish that paths with k peaks take k *left–turns* and $k - 1$ *right–turns*. Also, loops of t steps must take $\frac{t-2}{2} - (k-1)$ both *right–* and *left–steps*. Loops with $t = 2$ are different: they can only step away from the root and return to it in the next step (*left–turn*); their coefficient is $1 \times 1/\sqrt{3}$. Thus a simple loop with k peaks, for $t \geq 4$ steps, bears the coefficient:

$$\left(\frac{1}{\sqrt{3}} \right)^k \left(\frac{1 + a}{\sqrt{3}} \right)^{k-1} \left(\frac{a}{\sqrt{3}} \right)^{t/2-k} \left(\frac{2a}{\sqrt{3}} \right)^{t/2-k}$$

$$= \frac{1}{(\sqrt{3})^{t-1}} \left(\frac{1 + a}{2a^2} \right)^{k-1} (2a^2)^{t/2-1}$$

$$= \frac{1}{(\sqrt{3})^{t-1}} \left(\frac{-1}{2} \right)^{k-1} (2a^2)^{t/2-1} \quad (\text{as } a = e^{2\pi i/3}).$$

For $a = e^{2\pi i/3}$ we have $1 + a + a^2 = 0$, used above. Summed over all possible numbers of peaks k, and with $t = 2$ case added, the amplitude of a simple loop is

$$g(t) = \frac{1}{\sqrt{3}} \delta_0(t - 2)$$

$$+ \sum_{k=1}^{\frac{t-2}{2}} \frac{(2a^2)^{t/2-1}}{(\sqrt{3})^{t-1}} \left(\frac{-1}{2} \right)^{k-1} N\left(\frac{t - 2}{2}, k \right).$$

Using the Narayana numbers (13), with $t = 2m + 2$,

$$g(m) = \frac{1}{\sqrt{3}} \delta_0(m) + \frac{1}{m\sqrt{3}} \left(\frac{2a^2}{3} \right)^m$$

$$\times \sum_{k=0}^{m-1} \left(\frac{-1}{2} \right)^k \binom{m}{k + 1} \binom{m}{k}.$$

Since we will need the transform of $g(t)$, it is helpful to write the above sum as an integral, using the identity

$$\sum_{k=0}^{m-1} (\alpha\beta)^k \binom{m}{k + 1} \binom{m}{k} =$$

$$\frac{1}{2\pi} \int_0^{2\pi} \left(1 + \alpha e^{ix} \right)^m \left(1 + \beta e^{-ix} \right)^m \frac{e^{-ix}}{\alpha} dx.$$

Employing this, under the constraint $\alpha\beta = -1/2$,

$$g(m) = \frac{1}{\sqrt{3}}\,\delta_0(m) + \frac{1}{2\pi}\frac{1}{m\sqrt{3}}\left(\frac{2a^2}{3}\right)^m \qquad (14)$$
$$\times \int_0^{2\pi}\left(\frac{1}{2} + \alpha e^{ix} + \beta e^{-ix}\right)^m \frac{e^{-ix}}{\alpha}\,dx.$$

It is calculationally convenient to take the z–transform of $g(t)$ at this point. Since loops take even number of steps, and $\widehat{g}(z)_{t=0} = g(0) = 0$, with $t = 2m + 2$,

$$\widehat{g}(z) = \sum_{t=0}^{\infty} g(t)z^t = g(0) + g(2)z^2 + \sum_{t=4,6,\dots} g(t)z^t$$
$$= \widehat{g}(z)_{m=0} + \sum_{m=1}^{\infty} g(m)z^{2m+2}.$$

The transform of δ is 1, and Eq. (14) becomes

$$\widehat{g}(z) = \frac{1}{\sqrt{3}}z^2 + \frac{1}{2\pi\sqrt{3}}z^2\int_0^{2\pi} dx\,\frac{e^{-ix}}{\alpha}$$
$$\times\left[\sum_{m=1}^{\infty}\frac{1}{m}\left(\frac{2a^2}{3}\right)^m\left(\frac{1}{2} + \alpha e^{ix} + \beta e^{-ix}\right)^m z^{2m}\right].$$

Now we make use of $\sum_{n=1}^{\infty} x^n/n = -\ln(1-x)$, $|x| < 1$, and at this point pick $\alpha = -\beta = 1/\sqrt{2}$, arriving at

$$\widehat{g}(z) = \frac{z^2}{\sqrt{3}} + \frac{z^2}{2\pi}\sqrt{\frac{2}{3}}\int_0^{2\pi} dx\, e^{-ix}$$
$$\times\left\{-\ln\left[1 - z^2\frac{2a^2}{3}\left(\frac{1}{2} + \frac{e^{ix} - e^{-ix}}{\sqrt{2}}\right)\right]\right\}.$$

Using $\omega = e^{-ix}$ and integrating by parts,

$$\widehat{g}(z) = \frac{1}{\sqrt{3}}z^2 - z^4\frac{1}{2\pi i}\frac{2a^2}{3}$$
$$\times \oint_{|\omega|=1}\frac{\left(\frac{1}{\omega} + \omega\right) d\omega}{1 - \frac{2a^2 z^2}{3}\left(\frac{1}{2} + \frac{1}{\sqrt{2}}\left(\frac{1}{\omega} - \omega\right)\right)}.$$

Here the Residue Theorem is used. The singularity at $\omega = 0$ is removable, while one of the two zeros of the denominator is inside the integration contour. Finally,

$$\widehat{g}(z) = \frac{\sqrt{3}}{2a^2}\left[1 + \frac{1}{3}(az)^2 - \sqrt{1 - \frac{2}{3}(az)^2 + (az)^4}\right]. \quad (15)$$

This closed-form expression analytically extends $\widehat{g}(z)$ beyond the disk $|z| < 1$ on which it was defined. We now need to deal with $\widehat{h}_n(z)$.

Paths from the n-th level that reach the root for the first time in s steps, with amplitude $h_n(s)$, first reach the level $n - 1$, generally going out into the tree in the meanwhile, then the level $n-2$, and so forth until the root is hit. This is organized into paths dropping by one level closer to the root (with amplitude h_1), convoluted with the rest of the walk, which itself is comprised of paths getting closer to the root by one level, $h_n = h_1 * h_{n-1} = \dots = h_1 * \dots * h_1$ (n times). Then the transform is

$$\widehat{h}_n(z) = \left[\widehat{h}_1(z)\right]^n. \qquad (16)$$

Paths h_1, that for the first time reach one level closer to the root, are combinatorially equivalent to the paths that start at level 1 and touch the root for the first time.

Consider such a path, starting at level 1 and finding its way to the root for the first time, in more than one step (Fig. 4). It must have come to level 1 from level 2, and it first steps back to level 2. For comparison, now recall a root–to–root simple loop $g(s)$. It differs from h_1 by: the first step of g (with coefficient 1) is not taken by h_1 (which is already at level 1); and, the next step of g (for paths with $t > 2$) is a *right–step*, while the h_1 path takes a *right–turn*.
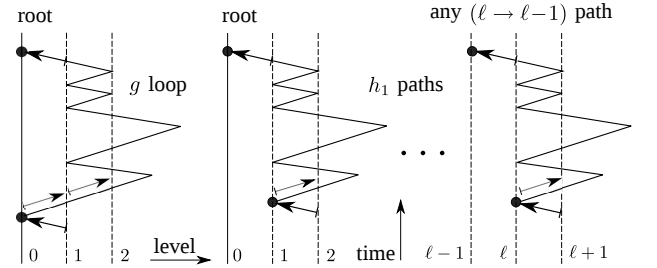

FIG. 4. Combinatorial comparison of root–to–root loops (g) and paths getting closer to root by one level (h_1), see text.

So we divide the expression for $g(s)$ by the coefficient associated with the second step of g that h_1 does not take, $2a/\sqrt{3}$, and multiply it by the coefficient of the step that h_1 takes instead, $(1 + a)/\sqrt{3}$. We also divide by the coefficient of the first step of g, not taken at all by h_1, which is 1. In the special case $s = 1$ a single step is taken to the root from the first level, with $a/\sqrt{3}$. Finally, this path takes one step more as compared to $g(s)$, so we use the expression for $g(s + 1)$, starting from $s = 3$ since $g(2)$ corresponds to the special case $h_1(1)$. This gives us the expression for the amplitude h_1,

$$h_1(s) = \frac{a}{\sqrt{3}}\delta_0(s - 1) + \frac{\frac{1+a}{\sqrt{3}}}{1 \times \frac{2a}{\sqrt{3}}}\,g(s+1) \times \mathbb{1}_{s\in\{3,5,\dots\}}.$$

Its transform is, using $1 + a + a^2 = 0$ (as $a = e^{2\pi i/3}$),

$$\widehat{h}_1(z) = \frac{a}{\sqrt{3}}\,z + \frac{1+a}{2a}\left[\frac{1}{z}\sum_{t=3,5,\dots} z^{t+1}g(t+1)\right] \qquad (17)$$
$$= \frac{a\,z}{\sqrt{3}} - \frac{a}{2\,z}\left(\widehat{g}(z) - \frac{z^2}{\sqrt{3}}\right) = \frac{a\sqrt{3}}{2}\,z - \frac{a}{2}\,\frac{\widehat{g}(z)}{z}.$$

The sum is the transform of $g(t \geq 4)$ $\left[\widehat{g}_{t\geq 4}\right]$, written as $\widehat{g} - \widehat{g}_{t=2}$. With Eqs. (12), (16), and (17), the generating

function for the amplitude of the process at the root is

$$\widehat{H}_n(z) = \left[-\frac{a}{2}\right]^n \left[\frac{\widehat{g}(z) - \sqrt{3}\,z^2}{z}\right]^n \frac{1}{1 - \widehat{g}(z)}, \qquad (18)$$

with $\widehat{g}(z)$ given in Eq. (15). Now we need to invert this.

B. Inverse transform: $H_n(t)$ asymptotic

We take the inverse z–transform via an integral, and using Laurent expansion and Residue Theorem,

$$H_n(t) = \frac{1}{2\pi i} \oint_{|z|=r<1} \frac{\widehat{H}_n(z)}{z^{t+1}} dz$$

$$= \frac{1}{2\pi i} \left[-\frac{a}{2}\right]^n \oint \frac{1}{z^{t+1}} \left[\frac{\widehat{g}(z) - \sqrt{3}\,z^2}{z}\right]^n \frac{dz}{1 - \widehat{g}(z)}.$$

This integral is too complicated to yield a closed-form solution. We look for its asymptotic behavior in the form

$$H_n(t) = \frac{(-a)^n}{2\pi i} \frac{1}{2^n} \oint_{|z|=r} \frac{\left[\widehat{g}(z) - \sqrt{3}\,z^2\right]^n}{1 - \widehat{g}(z)} \frac{dz}{z^{t+n+1}}, \quad (19)$$

using the steepest descent method. The calculation is discussed in Appendix A. The asymptotic of the amplitude of the process at the root, starting from a level n in the tree, with $\tau \equiv t - n$, is

$$H_n(t) \sim \frac{(-a)^n}{2\pi i} \frac{1}{2^n} \times (\sqrt{2})^n (-1)^n \qquad (20)$$

$$\times \left[c_{1n}\, e^{-i\gamma n} \frac{e^{-i\lambda_1 \frac{\tau}{2}}}{\tau^{3/2}} - c_{2n}\, e^{i\gamma n} \frac{e^{-i\lambda_2 \frac{\tau}{2}}}{\tau^{3/2}} \right].$$

Constants c_{1n} and c_{2n} are linear in n, while γ and λ's are real constants (Appendix A). The probability is

$$|H_n(t)|^2 \sim \frac{C^2 - 2\,\mathrm{Re}\left\{c_1 c_2^* \, e^{-i\left[2\gamma n + (\lambda_1 - \lambda_2)\frac{\tau}{2}\right]}\right\}}{4\pi^2\, 2^n\, \tau^3}, \quad (21)$$

where $C^2 = |c_1|^2 + |c_2|^2 \sim n^2$. The oscillations of the exponential term are rapid at large times (and/or n), and this function behaves as $\sim \tau^{-3}$. The n dependence is $\sim n^2/2^n$ at large times. Also, we see that the walk is transient, in the sense introduced in [39, 40], since $\sum_t^\infty |H_n(t)|^2$ is finite.

The observed power law decay differs sharply from the exponential tail of the classical walk (Appendix B). On finite graphs built with binary trees, this exponentially slower decay may lead to algorithms with significant speedups. The treatment in this section is meant to lay the groundwork for such investigations.

This behavior should also have general implications for physics of systems modeled with a binary tree.

C. Inverse transform: $H_n(t)$ computed

The transform is defined as $\widehat{H}_n(z) = \sum_{t \geq n} H_n(t) z^t$, and using its Taylor expansion and equating coefficients,

$$H_n(t) = \frac{\widehat{H}_n^{(t)}(z)|_{z=0}}{t!}. \qquad (22)$$

This can be evaluated efficiently, for a range of values of t for a fixed n, providing the full amplitude. Symbolic calculation of derivatives (with MATHEMATICA) allows for values of n in the thousands. We note that the amplitude shows an interference pattern, with the main peak followed by (much) smaller, rapidly diminishing, secondary peaks. Probability at the root with time is shown in Fig. 5, for $n = 50$. The shape does not depend on n. At long times this exact result can be compared with asymptotics (21), see inset in Fig. 5. The tail exhibits t^{-3} dependence, in agreement with Eq. (21).
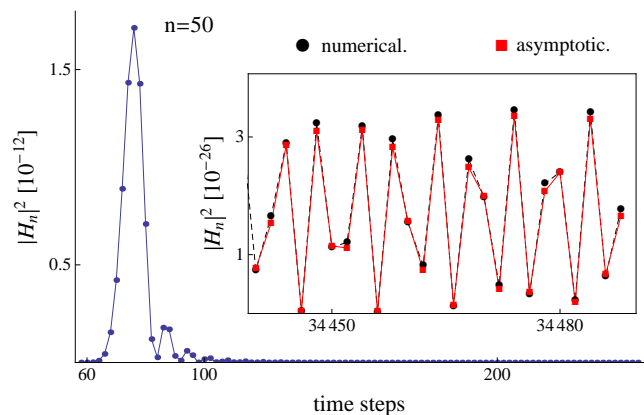
FIG. 5. Probability at the root with time ($n = 50$), computed via Eq. (22). Inset compares this (points) with the steepest descent asymptotic (21) at same time steps (red squares).

D. Comparison and algorithmic aspects

We considered an algorithm of finding the root starting at the n–th generation in the tree. Here we compare the quantum and classical walks, and their estimated run times, using data calculated via Eqs. (22) and (B3). Probability peaks and times at which they are reached, for quantum and classical walks, are shown in Table I for a few initial levels n. Probability at the root for the classical walk is shown in Fig. 6.

The best run time for a given n is estimated as follows. The inverse of the probability is the average number of times needed to run in order to hit the root; multiplying it by its time gives the total running time to hit the root. We need its minimum over all time steps, $\min\{t/|H_n(t)|^2\}$, usually the values for the peak. We use data up to $n = 5000$ in steps of 100 for the quantum

initial level n	10	20	50	100	200	500
max $|H_n|^2$ (at t)	6.8×10^{-4} (16)	3.9×10^{-6} (30)	1.7×10^{-12} (76)	5.3×10^{-23} (150)	7.6×10^{-44} (298)	5.1×10^{-106} (738)
max $p_t(n)$ (at t)	1.2×10^{-4} (22)	7.2×10^{-8} (52)	4.2×10^{-17} (142)	2.6×10^{-32} (292)	1.4×10^{-62} (592)	4.5×10^{-153} (1492)

TABLE I. Probability peaks at the root with their times, for quantum $\left[|H_n(t)|^2\right]$ and classical $\left[p_t(n,0)\right]$ walks, with n.
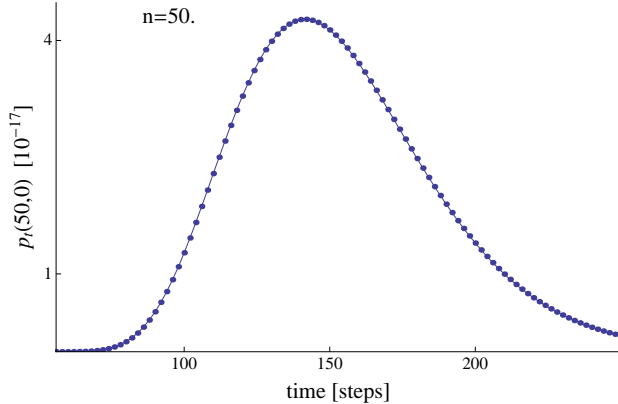
FIG. 6. Classical walk, probability at the root. Appendix B.

walk, and up to $n = 2000$ in steps of 50 for the classical walk (numerical integration is more demanding). Using smaller increments in n does not affect the results. Log of run times is fit with a polynomial and linear (Fig. 7).
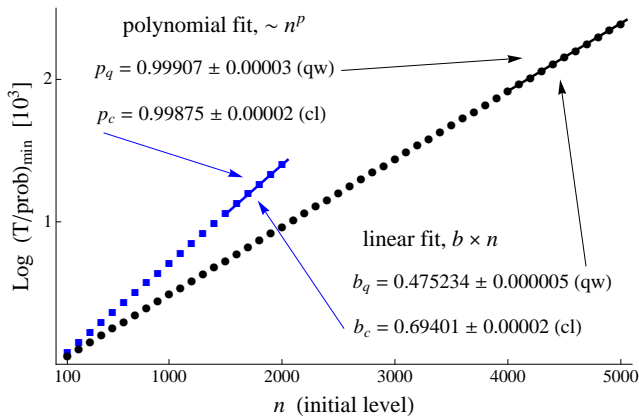
FIG. 7. Log of run time with initial level in the tree, for quantum (points) and classical (blue squares) walks. For plot clarity not all points are shown. Parameter values for polynomial ($\sim n^p$) and linear (bn) fits are shown, with lines through data used for fits, see text. The run time is $\sim e^{bn}$, and $b_q/b_c \to 2/3$ estimates the quantum over classical walk speedup.

The polynomial fit establishes a linear trend (reached at $n \sim$ a few hundred), so the run time of the quantum walk is exponential in the initial distance from the root, $\sim e^{bn}$. The same holds for the classical walk, and then the ratio of slopes of their linear fits compares their run times.

This ratio does not change much over the whole range of data, being within a few percent of $2/3$. Still, since an

exponential complexity is fully felt at large n, the later portions of data are more relevant for algorithmic comparison. For the last quarter of data ranges, indicated in Fig. 7 by lines fit through data, the ratio of quantum to classical slopes is ≈ 0.685, within 3% of $2/3$. Thus it appears reasonable to conjecture the algorithmic speedup of the order of $2/3$. (For a run time T for the classical walk, one expects the run time on the order of $T^{2/3}$ for the quantum walk.)

We note the behavior of peaks' times with n. For the classical walk, $t_{\max}^{cl}(n) = 3n - 8$ (exact), while for the quantum walk $t_{\max}^{qw}(n) \approx 1.46n$ (where data allows for a fit $\sim 1.5n$, and for a $\sim \log n$ correction).

IV. CONCLUDING REMARKS

Quantum walks are quantum processes with a specific mixing of states; particular unitary processes. In this vein, we propose to approach and study them using ideas from classical random walks with memory.

We have demonstrated how a general framework for discrete-time quantum walks arises as a natural analog of a specific representation of a classical memory–2 Markov chain. Walks are implemented by constructing a local operator with no restrictions other than unitarity. The framework needs no "coin" degrees of freedom, is flexible, and applicable to general graphs. This approach may make it easier to obtain walks on structures for which significant speedups are expected.

The evolution operator works separately on each component of the amplitude, reducing the state space, and effectively deconstructing the amplitude [as in in the binary tree example, Eqs. (7–9)]. This makes quantum-mechanical correlations and interference transparent in quantum walks, making their explicit study easier. It should also aid the use of quantum walks as a general tool for exploration and modeling of physical systems.

In Sec. III we use the framework to build a symmetric discrete-time quantum walk on a semi-infinite binary tree. We start the walk at a level n in the tree, and find its amplitude at the root as a function of time and n. The construction of the walk is simple, but the calculation is complicated by a (reflective) boundary. The generating function of the amplitude is found explicitly, and its asymptotic is found via the steepest descent method. The full solution is computed numerically.

These solutions show interesting features. The asymptotic decays in time by the power law (as opposed to the exponential tail of the classical walk), representing long–

range correlations. This hints at significant speedups on restricted structures. The amplitude exhibits a damped interference pattern, with a distinct and sharp peak. In comparison with the classical walk, the probability peak is reached quicker in time, and is orders of magnitude greater, already at small n. The run time for hitting the root on a semi-infinite binary tree is exponential with n for the quantum walk, as it is for the classical walk. It is still clearly slower in n and, following suggestive data trends, we conjecture the polynomial algorithmic speedup of the order of $2/3$ over a classical walk.

Appendix A: Steepest descent calculation summary

Integrals suitable for analysis by the steepest descent method are typically of the form [41]

$$I(k) = \int_C f(\omega)\, e^{k\Phi(\omega)}\, d\omega. \qquad (A1)$$

We use Eq. (19), where the exponent will be formed from powers of z. As z is always squared we first change variables via $z^2 = \xi$. Accounting for the double winding,

$$I(t;n) = 2 \times \frac{1}{2} \oint_{|\sqrt{\xi}|=r} \frac{\left[\frac{\widehat{g}(\xi)}{\xi} - \sqrt{3}\right]^n}{1 - \widehat{g}(\xi)} \frac{1}{\xi}\, \frac{d\xi}{\xi^{\frac{t-n}{2}}}.$$

We now use $\widehat{g}(\xi)/\xi = \omega$, to transfer some of the integrand's complexity into the exponent,

$$\frac{\widehat{g}(\xi)}{\xi} = \omega, \quad \xi = \varphi(\omega) = a\sqrt{3}\, \frac{\omega - \frac{1}{\sqrt{3}}}{(\omega + \frac{1}{\sqrt{3}})(\omega - \frac{2}{\sqrt{3}})}.$$

Carrying out the substitution, we have

$$I(t;n) = \oint_{|\sqrt{\varphi}|=r} \frac{(\omega - \sqrt{3})^n}{(1 - \omega\,\varphi)} \frac{\varphi\prime}{\varphi}\, \varphi^{-\frac{t-n}{2}}\, d\omega, \qquad (A2)$$

in the form (A1), with $\varphi^{-\frac{t-n}{2}} = e^{\frac{t-n}{2}\log(\varphi^{-1})}$, and

$$f = \frac{(\omega - \sqrt{3})^n}{(1 - \omega\,\varphi)} \frac{\varphi\prime}{\varphi}, \quad \Phi = -\log\varphi, \quad k = \frac{t-n}{2}. \quad (A3)$$

Keeping φ'/φ will be useful. Consider the critical points. A pole of order $\frac{t-n+2}{2}$ is at $\varphi = 0 \Rightarrow \omega_p = 1/\sqrt{3}$. Two simple poles are at $-\frac{1}{\sqrt{3}}$, $\frac{2}{\sqrt{3}}$. The logarithm's branch point is at $\varphi = 1$, and since this is not at $\omega_p = 1/\sqrt{3}$, what the contour must enclose, we can take any convenient branch. Two simple saddle points are

$$(\log\varphi)\prime = 0 \;\Rightarrow\; \omega_{s1/s2} = \frac{1 \pm i\sqrt{2}}{\sqrt{3}} = e^{\pm i\arctan\sqrt{2}}.$$

The main contribution to this integral comes from saddle points. A branch of the original integration contour $|\sqrt{\varphi}| = r$ can be chosen (via r) for use with steepest descent paths. There are no issues with deforming the
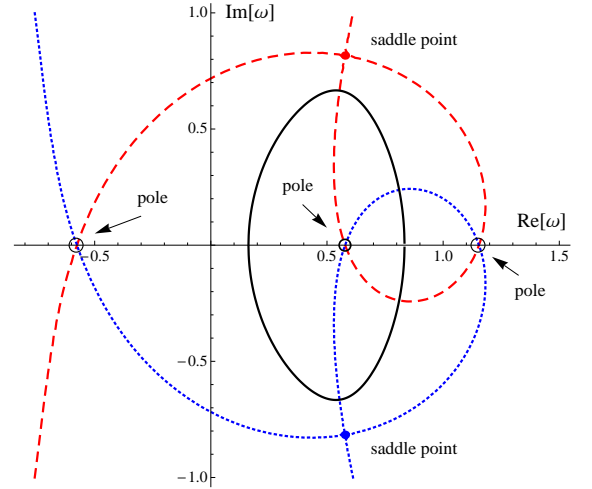

FIG. 8. Original integration contour (solid), steepest descent paths (dashed and dotted), and critical points.

contour, as no critical points are in the way, any branch of the logarithm is good, and $k = \frac{t-n}{2} \in \mathbb{Z}$ (Fig. 8).

In the steepest descent method decreasing orders of contribution are computed mostly via expansion around saddles. (There are theorems and formulas for the first–order contribution, but here it is zero.) Around ω_s we have $\Phi(\omega) = \Phi(\omega_s) + \frac{1}{2!}\left[\Phi(\omega)\right]''_{\omega_s}(\omega - \omega_s)^2 + o(\omega^2)$, and the usual change of variables $\Phi(\omega) - \Phi(\omega_s) = -y$ gives

$$\omega = \mp b\sqrt{y} + \omega_s, \quad b = \sqrt{\frac{2}{\left[\log\varphi(\omega)\right]''_{\omega=\omega_s}}}, \qquad (A4)$$

where y is zero at the saddle and real along the steepest descent path. We used $\sqrt{(\log\varphi^{-1})''} = i\sqrt{(\log\varphi)''}$. Now $y = \log\left[\varphi(\omega)/\varphi(\omega_s)\right]$ and $dy = \left[\varphi(\omega)'/\varphi(\omega)\right]d\omega$, and with $\varphi(\omega) = \varphi(\omega_s)\,e^y$ the integral (A2–A3) becomes

$$I(k) \sim e^{k\Phi(\omega_s)} \oint \frac{\left[\omega(y) - \sqrt{3}\right]^n}{1 - \omega(y)\,\varphi(\omega_s)\,e^y}\, e^{-ky}\, dy. \qquad (A5)$$

Now we can directly expand around $y = 0$ (to any order), restricting integration to the line along the steepest descent path, close to saddles. The signs in Eq. (A4) correspond to the opposite directions from the saddle; we label $+/-$ as "R/L." Substituting $\omega(y)$ and expanding,

$$I \sim A\,\varphi_s^{-k} \int_0^\delta \left(1 \pm B\sqrt{y}\right) e^{-ky}\, dy, \quad \delta \sim o(1), \quad (A6)$$

$$A = \frac{\left[\omega_s - \sqrt{3}\right]^n}{1 - \omega_s\,\varphi_s}, \; B = \left(\frac{b\,\varphi_s}{1 - \omega_s\varphi_s} + \frac{b}{\omega_s - \sqrt{3}}\, n\right).$$

For compactness we use $\varphi_s \equiv \varphi(\omega_s) = e^{i\lambda_s}$, with $\lambda_{s1} = \arctan\left[(9\sqrt{3}+8\sqrt{2})/23\right]$, $\lambda_{s2} = \arctan\left[(9\sqrt{3}-8\sqrt{2})/23\right] - \pi$. Note that $A(n) \sim (\sqrt{2})^n$, as $\omega_s - \sqrt{3} = \sqrt{2}e^{i\gamma_s}$, with $\gamma_{s1/s2} = \mp\left[\arctan(1/\sqrt{2}) - \pi\right] \equiv \mp(\gamma - \pi)$, and we will extract π later. The integral is dominated around ω_s

($\delta \approx 0$), so it can be formally extended, $\delta \to \infty$, and we get $I \sim A \int_0^\infty \left(1 \pm B\sqrt{y}\right) e^{-ky} \, dy$. This results in

$$I_{R/L}(k;n) \sim A_n \left(\frac{1}{k} \pm \frac{\sqrt{\pi}}{2} \frac{B_n}{k\sqrt{k}}\right) \varphi(\omega_s)^{-k}. \quad \text{(A7)}$$

Subtracting contributions along opposite directions, the first non–zero order for either saddle is

$$I_s \sim (\sqrt{2})^n e^{i\gamma_s n} (a_s + d_s n) \frac{e^{-i\lambda_s k}}{k\sqrt{k}}. \quad \text{(A8)}$$

We broke up the $A_n B_n$ term found in $I_R - I_L$, to show the structure of n dependence, where $a_s = \frac{b\varphi_s\sqrt{\pi}}{(1-\omega_s\varphi_s)^2}$ and $d_s = \frac{b\sqrt{\pi}}{(1-\omega_s\varphi_s)(\omega_s-\sqrt{3})}$ are of order ~ 1. Here we extract π from γ_s, and will use $e^{i\gamma_s} = (-1)e^{\mp i\gamma}$. Contributions for saddles are subtracted (for consistency of $\pm\sqrt{y}$ directions) and, with $c_{s,n} \equiv a_s + d_s n$, we get Eq. (20).

The full expansion of the integral (A5) results in nested sums of a Gamma function. This cannot capture the peak of the amplitude though, and is not needed for our asymptotic analysis, so we do not pursue it here.

Appendix B: Random walk on a semi-infinite line

For completeness here we provide the application of the method developed in [42, 43] (based on Karlin-McGregor spectral approach to random walks) to a classical walk on a binary tree.

If P is a reversible Markov chain over a sample space Ω, and π is a reversibility function (not necessarily a probability distribution), then P is a self-adjoint operator in $\ell^2(\pi)$, the space generated by the inner product

$$< f, g >_\pi = \sum_{x \in S} f(x) g(x) \pi(x)$$

induced by π. If P is tridiagonal operator (i.e. a nearest-neighbor random walk) on $\Omega = \{0, 1, 2, \dots\}$, then it must have a simple spectrum, and is diagonalizable via orthogonal polynomials as it was studied in the 50's and 60's by Karlin and McGregor. There the extended eigenfunctions $Q_j(\lambda)$ ($Q_0 \equiv 1$) are orthogonal polynomials with respect to a probability measure ψ and

$$p_t(i,j) = \pi_j \int_{-1}^1 \lambda^t Q_i(\lambda) Q_j(\lambda) d\psi(\lambda) \quad \forall i, j \in \Omega,$$

where π_j ($\pi_0 = 1$) is the reversibility measure of P. Consider the following Markov chain

$$P = \begin{pmatrix} 0 & 1 & 0 & 0 & \dots \\ q & 0 & p & 0 & \dots \\ 0 & q & 0 & p & \ddots \\ \vdots & \vdots & \ddots & \ddots & \ddots \end{pmatrix} \qquad p > q.$$

Orthogonal polynomials are obtained via solving a simple linear recursion: $Q_0 = 1$, $Q_1 = \lambda$, and

$$Q_n(\lambda) = c_1(\lambda)\rho_1^n(\lambda) + c_2(\lambda)\rho_2^n(\lambda),$$

where $\rho_1(\lambda) = \frac{\lambda + \sqrt{\lambda^2 - 4pq}}{2p}$ and $\rho_2(\lambda) = \frac{\lambda - \sqrt{\lambda^2 - 4pq}}{2p}$ are the roots of the characteristic equation for the recursion, and $c_1 = \frac{\rho_2 - \lambda}{\rho_2 - \rho_1}$ and $c_2 = \frac{\lambda - \rho_1}{\rho_2 - \rho_1}$. Now $\pi_0 = 1$ and $\pi_n = \frac{p^{n-1}}{q^n}$ ($n \geq 1$). Also, we observe that

$$\begin{aligned} |\rho_2(\lambda)| &> \sqrt{q/p} \quad \text{on } [-1, -2\sqrt{pq}), \\ |\rho_2(\lambda)| &< \sqrt{q/p} \quad \text{on } (2\sqrt{pq}, 1], \\ |\rho_2(\lambda)| &= \sqrt{q/p} \quad \text{on } [-2\sqrt{pq}, 2\sqrt{pq}], \end{aligned}$$

and $\rho_1\rho_2 = \frac{q}{p}$. The above will help us to identify the point mass locations in the measure ψ since each point mass in ψ occurs when $\sum_k \pi_k Q_k^2(\lambda) < \infty$. Thus we need to find all $\lambda \in (2\sqrt{pq}, 1]$ such that $c_1(\lambda) = 0$ and all $\lambda \in [-1, -2\sqrt{pq})$ such that $c_2(\lambda) = 0$. But there are no such roots, as $c_1(-1) = 0$ and $c_2(1) = 0$, while $-1 \notin (2\sqrt{pq}, 1]$ and $1 \notin [-1, -2\sqrt{pq})$. Thus there are no point mass atoms in ψ, and the mass of ψ must be continuously distributed inside $[-2\sqrt{pq}, 2\sqrt{pq}]$. In order to find the density of ψ inside $[-2\sqrt{pq}, 2\sqrt{pq}]$ we need to find $(e_0, (P - sI)^{-1}e_0)$ for $\text{Im}(s) \neq 0$, i.e. the upper left element in the resolvent of P.

Let $(a_0(s), a_1(s), \dots)^T = (P - sI)^{-1}e_0$, then

$$-sa_0 + a_1 = 1, \quad \text{and} \quad qa_{n-1} - sa_n + pa_{n+1} = 0$$

Thus $a_n(s) = \alpha_1\rho_1(s)^n + \alpha_2\rho_2(s)^n$, with $\alpha_1 = \frac{a_0(\rho_2 - s) - 1}{\rho_2(s) - \rho_1(s)}$ and $\alpha_2 = \frac{1 - a_0(\rho_1 - s)}{\rho_2(s) - \rho_1(s)}$. Since $(a_0, a_1, \dots) \in \ell^2(\mathbb{C}, \pi)$,

$$|a_n|\sqrt{\frac{p^n}{q^n}} \to 0 \qquad \text{as} \quad n \to +\infty$$

Hence when $|\rho_1(s)| \neq |\rho_2(s)|$, either $\alpha_1 = 0$ or $\alpha_2 = 0$, and therefore

$$a_0(s) = \frac{\mathbb{1}_{|\rho_1(s)| < \sqrt{\frac{q}{p}}}}{\rho_1(s) - s} + \frac{\mathbb{1}_{|\rho_2(s)| < \sqrt{\frac{q}{p}}}}{\rho_2(s) - s}. \quad \text{(B1)}$$

Also $d\psi(z) = \varphi(z)dz$, where $\varphi(z)$ is an atom-less density function over $[-2\sqrt{pq}, 2\sqrt{pq}]$, and

$$a_0(s) = \int_{-2\sqrt{pq}}^{+2\sqrt{pq}} \frac{d\psi(z)}{z - s} = \int_{-2\sqrt{pq}}^{+2\sqrt{pq}} \frac{\varphi(z)dz}{z - s}.$$

Next we will use the following basic property of Cauchy transforms $Cf(s) = \frac{1}{2\pi i} \int_\mathbb{R} \frac{f(z)dz}{z-s}$ that can be derived using the Cauchy integral formula, or similarly, an approximation to the identity formula:

$$C_+ - C_- = I. \quad \text{(B2)}$$

Observe that the curve in the integral need not be in $\mathbb{R}$ for $C_+ - C_- = I$ to hold. Here

$$C_+ f(z) = \lim_{\substack{s \to z:\ \mathrm{Im}(s)>0}} Cf(s), \quad \text{and}$$

$$C_- f(z) = \lim_{\substack{s \to z:\ \mathrm{Im}(s)<0}} Cf(s),$$

for all $z \in \mathbb{R}$. The relation (B2) implies

$$\varphi(x) = \frac{1}{2\pi i} \left(\lim_{\substack{s=x+i\varepsilon:\\ \varepsilon \to 0+}} a_0(s) - \lim_{\substack{s=x-i\varepsilon:\\ \varepsilon \to 0+}} a_0(s) \right),$$

for all $x \in (-2\sqrt{pq}, 2\sqrt{pq})$. Recalling (B1), we express φ as $\varphi(x) = \frac{\rho_1(x) - \rho_2(x)}{2\pi i (\rho_1(x) - x)(\rho_2(x) - x)}$ for $x \in (-2\sqrt{pq}, 2\sqrt{pq})$, which in turn simplifies to

$$\varphi(x) = \begin{cases} \frac{\sqrt{4pq - x^2}}{2\pi q(1 - x^2)} & \text{if } x \in (-2\sqrt{pq}, 2\sqrt{pq}), \\ 0 & \text{otherwise.} \end{cases}$$

Here $\varphi(x)$ always integrates to 1 over $(-2\sqrt{pq}, 2\sqrt{pq})$.

Now

$$p_t(n, 0) = \int_{-2\sqrt{pq}}^{+2\sqrt{pq}} \lambda^t Q_n(\lambda) \varphi(\lambda) d\lambda$$

$$= \int_{-2\sqrt{pq}}^{+2\sqrt{pq}} \lambda^t (c_1 \rho_1^n + c_2 \rho_2^n) \frac{(\rho_1 - \rho_2)\, d\lambda}{2\pi i (\rho_1 - \lambda)(\rho_2 - \lambda)},$$

and therefore, since $c_1 = \frac{\rho_2 - \lambda}{\rho_2 - \rho_1}$ and $c_2 = \frac{\lambda - \rho_1}{\rho_2 - \rho_1}$,

$$p_t(n, 0) = \frac{1}{2\pi i} \int_{-2\sqrt{pq}}^{+2\sqrt{pq}} \lambda^t \left(\frac{\rho_2^n}{\rho_2 - \lambda} - \frac{\rho_1^n}{\rho_1 - \lambda} \right) d\lambda. \quad \text{(B3)}$$

This can be treated as a complex integral, for example with steepest descent. But one can observe directly in Eq.(B3) that the tail of $p_t(n, 0)$ decays as $(2\sqrt{pq})^t$ when $t \to +\infty$. Thus, using $p = 2/3$ and $q = 1/3$ for the classical symmetric walk on the semi-infinite binary tree, the decay rate will be $(2\sqrt{2}/3)^t$, giving us the exponential asymptotics. The probability integral (B3) can be efficiently evaluated numerically, see Fig. 6.

[1] D. A. Meyer, J. Stat. Phys. **85**, 551 (1996).
[2] Y. Shikano, K. Chisaki, E. Segawa, and N. Konno, Phys. Rev. A **81**, 062129 (2010).
[3] X. Martin, D. O'Connor, and R. D. Sorkin, Phys. Rev. D **71**, 024029 (2005).
[4] O. Mülken, A. Blumen, T. Amthor, C. Giese, M. Reetz-Lamour, and M. Weidemüller, Phys. Rev. Lett. **99**, 090601 (2007); A. Thilagam, Phys. Rev. A **81**, 032309 (2010).
[5] T. Kitagawa, M. S. Rudner, E. Berg, and E. Demler, Phys. Rev. A **82**, 033429 (2010).
[6] O. Mülken and A. Blumen, Phys. Rept. **502**, 37 (2011).
[7] A. M. Childs, Phys. Rev. Lett. **102**, 180501 (2009).
[8] E. Farhi and S. Gutmann, Phys. Rev. A **58**, 915 (1998).
[9] J. Watrous, J. Comput. Syst. Sci. **62**, 376 (2001).
[10] Y. Aharonov, L. Davidovich, and N. Zagury, Phys. Rev. A **48**, 1687 (1993).
[11] A. Ambainis, E. Bach, A. Nayak, A. Vishwanath, and J. Watrous, in *Proceedings of the 33rd Annual ACM Symposium on Theory of Computation*, STOC '01 (ACM, New York, 2001) pp. 37–49.
[12] D. Aharonov, A. Ambainis, J. Kempe, and U. Vazirani, in *Proceedings of the 33rd Annual ACM Symposium on Theory of Computation*, STOC '01 (ACM, New York, 2001) pp. 50–59.
[13] A. M. Childs, R. Cleve, E. Deotto, E. Farhi, S. Gutmann, and D. A. Spielman, in *Proceedings of the 35th Annual ACM Symposium on Theory of Computation*, STOC '03 (ACM, New York, 2003) pp. 59–68.
[14] A. M. Childs, L. J. Schulman, and U. V. Vazirani, in *Foundations of Computer Science, 2007. FOCS '07. 48th Annual IEEE Symposium on* (2007) pp. 395 –404.
[15] C. A. Ryan, M. Laforest, J. C. Boileau, and R. Laflamme, Phys. Rev. A **72**, 062317 (2005); H. Schmitz, R. Matjeschk, C. Schneider, J. Glueckert, M. Enderlein, T. Huber, and T. Schaetz, Phys. Rev. Lett. **103**, 090504 (2009); M. Karski, L. Förster, J.-M. Choi, A. Steffen, W. Alt, D. Meschede, and A. Widera, Science **325**, 174 (2009); A. Schreiber, K. N. Cassemiro, V. Potoček, A. Gábris, P. J. Mosley, E. Andersson, I. Jex, and C. Silberhorn, Phys. Rev. Lett. **104**, 050502 (2010); F. Zähringer, G. Kirchmair, R. Gerritsma, E. Solano, R. Blatt, and C. F. Roos, Phys. Rev. Lett. **104**, 100503 (2010); M. A. Broome, A. Fedrizzi, B. P. Lanyon, I. Kassal, A. Aspuru-Guzik, and A. G. White, Phys. Rev. Lett. **104**, 153602 (2010); A. Peruzzo *et al.*, Science **329**, 1500 (2010); A. Schreiber, K. N. Cassemiro, V. Potoček, A. Gábris, I. Jex, and C. Silberhorn, Phys. Rev. Lett. **106**, 180403 (2011).
[16] J. Kempe, Contemp. Phys. **44**, 307 (2003).
[17] A. M. Childs, Commun. Math. Phys. **294**, 581 (2009).
[18] M. Szegedy, in *Proceedings of the 45th Annual IEEE Symposium on Foundations of Computer Science* (IEEE Computer Society, Washington, DC, 2004) pp. 32–41.
[19] B. Tregenna, W. Flanagan, R. Maile, and V. Kendon, New J. Phys. **5**, 83 (2003).
[20] A. Romanelli, A. Schifino, R. Siri, G. Abal, A. Auyuanet, and R. Donangelo, Physica A **338**, 395 (2004).
[21] C. M. Chandrashekar, R. Srikanth, and R. Laflamme, Phys. Rev. A **77**, 032326 (2008).
[22] P. Xue, B. C. Sanders, and D. Leibfried, Phys. Rev. Lett. **103**, 183602 (2009).
[23] D. A. Meyer and H. Blumer, J. Stat. Phys. **107**, 225 (2002).
[24] N. Konno, Stochastic Models **25**, 28 (2009).
[25] F. W. Strauch, Phys. Rev. A **74**, 030301 (2006).
[26] This representation is not explored in the literature.
[27] T. A. Brun, H. A. Carteret, and A. Ambainis, Phys. Rev. A **67**, 052317 (2003); Phys. Rev. A **67**, 032304 (2003).
[28] J. Košík, V. Bužek, and M. Hillery, Phys. Rev. A **74**,

022310 (2006).

[29] M. Mc Gettrick, Quantum Inf. Comput. **10**, 0509 (2010); N. Konno and T. Machida, **10**, 1004 (2010).

[30] M. Hillery, J. Bergou, and E. Feldman, Phys. Rev. A **68**, 032314 (2003).

[31] E. Feldman and M. Hillery, Phys. Lett. A **324**, 277 (2004).

[32] D. Reitzner, M. Hillery, E. Feldman, and V. Bužek, Phys. Rev. A **79**, 012323 (2009).

[33] M. Hillery, D. Reitzner, and V. Bužek, Phys. Rev. A **81**, 062324 (2010).

[34] E. Feldman, M. Hillery, H.-W. Lee, D. Reitzner, H. Zheng, and V. Bužek, Phys. Rev. A **82**, 040301 (2010).

[35] U_j implements (one-step) memory by acting on the originating site, it can be interpreted as a scattering operator on j, and it mixes components (à la coined walks).

[36] For instance: E. Farhi, J. Goldstone, and S. Gutmann, Theory Comput. **4**, 169 (2008); Y.-Y. Shi, L.-M. Duan, and G. Vidal, Phys. Rev. A **74**, 022320 (2006); P. Reben-trost, M. Mohseni, I. Kassal, S. Lloyd, and A. Aspuru-Guzik, New J. Phys. **11**, 033003 (2009); P. Silvi, V. Giovannetti, S. Montangero, M. Rizzi, J. I. Cirac, and R. Fazio, Phys. Rev. A **81**, 062335 (2010).

[37] For a mixed state at j, U_j acts on each originating state, $\widehat{U}\,\widehat{X}\,|\psi\rangle^{(j)} = \widehat{U}\,\widehat{X} \sum_{i \in S} c_{ij}\,|i\rangle \otimes |j\rangle = \sum_{i \in S} c_{ij}\,|j\rangle \otimes U_j|i\rangle$, fully specifying propagation over site j. We only need the evolution step of a pure state for this calculation.

[38] P. A. MacMahon, *Combinatorial Analysis, Vols. 1 and 2* (Cambridge University Press, 1915).

[39] M. Štefaňák, I. Jex, and T. Kiss, Phys. Rev. Lett. **100**, 020501 (2008); M. Štefaňák, T. Kiss, and I. Jex, Phys. Rev. A **78**, 032306 (2008).

[40] M. Cantero, L. Moral, F. A. Grünbaum, and L. Velzquez, Commun. Pure Appl. Math. **63**, 464 (2010), arXiv:0901.2244.

[41] R. Wong, *Asumptotic Approximations of Integrals* (Academic Press, 1989); N. Bleistein and R. A. Handelsman, *Asymptotic expansions of integrals* (Dover, 1986).

[42] Y. Kovchegov, Elect. Comm. in Probab. **14**, 90 (2009).

[43] Y. Kovchegov, Elect. Comm. in Probab. **15**, 59 (2010).